Study of beam echoes in the IOTA ring

Lee Teng Fellowship in Accelerator Science and Engineering

Dhruv Desai, University of Illinois at Urbana-Champaign

Mentor: Tanaji Sen, Fermilab

Abstract

This study covers simulation of transverse beam echoes in the IOTA ring, and testing the effects different beam and ring parameters have on their properties. Using MADX and C++ to simulate and analyze a proton beam passing through the IOTA (Integrable Optics Test Accelerator) lattice, it was found that echoes of reasonable amplitudes and widths were produced that obey the nonlinear echo theory. New results on effects of coupling were observed. Impact of misalignment and gradient errors was analyzed to test practicality of echo generation in the IOTA ring. Multiple echoes were observed to gather more accurate results on diffusion. Findings from this study will help test integrability of the IOTA ring via quick diffusion measurements.

1 Introduction

Beam diffusion is a consequence of intensity, space charge, beam-beam interaction, and many other effects. It can cause emittance growth, and lead to loss of particles. Hence, in order to keep track of beam evolution in phase space, it is important to measure diffusion. The current method requires scraping the beam using a collimator, retracting the collimator, and allowing the beam to diffuse to the outer position of the jaws[1]. The main disadvantage of this method is that it takes hours to measure diffusion. An effective alternative is to use transverse beam echoes, which can achieve the same task in milliseconds of time.

Echo amplitudes and widths strongly depend on diffusion rates of the beam, along with other parameters such as tunes, coupling, chromaticity, etc. By studying echo dependences on these parameters, it is possible to use the nonlinear echo theory to measure diffusion coefficients. However, the current theory of echoes is developed in one dimension and fails to take into account effects of coupling, which needs to be understood in order to improve the accuracy of calculations.

Using simulations of the beam passing through the IOTA lattice, we confirm the 1-D nonlinear echo theory, test robustness of dynamic aperture and echoes against choice of tunes, longitudinal momentum spread and misalignment and gradient errors, and study echo dependences on coupling to construct a complete 2-D theory of echoes. The end goal is to achieve echoes with properties practical enough for diffusion measurements.

2 What is a beam echo?

A beam echo is a recoherence of particles in phase space, following phase decoherence due to presence of nonlinear elements in the lattice. We describe the particle motion using coordinates in Floquet phase space.

$$\xi = \frac{x}{\sqrt{\beta}} \qquad \eta = \frac{\sqrt{\beta}}{x} + \frac{\alpha}{\sqrt{\beta}} x^{'} \tag{1}$$

x and $x^{'}$ are position and normalized momentum respectively, and α and β are the usual Courant-Snyder parameters. In the absence of nonlinearities in the ring, the particles form a circle in the Floquet phase space, where action, defined as

$$J = \frac{\xi^2 + \eta^2}{2} \tag{2}$$

is conserved. However, in the presence of nonlinear elements (e.g. sextupoles or octupoles), the action is no longer conserved and a nonlinear tune spread occurs in particles, which is responsible for the decoherence and recoherence of particle motion in phase space.

Suppose a steady beam is kicked in the transverse direction using a dipole kicker at time $t = 0$. All the particles oscillate about the nominal trajectory with larger amplitudes (dipole kick increases the energy, and thus the amplitude of oscillations of particles). Since the particles are initially in phase with one another, the centroid also oscillates with large amplitudes. However, the tune spread causes particles to go out of phase as time passes, causing beam decoherence, and even though individual particles keep executing

betatron oscillations with large amplitudes, the overall centroid oscillation asymptotically drops down to zero. The drop rate can be characterized using **decoherence time**, defined as the time when the centroid signal drops to $1/e$ times its initial value. Long after the beam has decohered, it is kicked again with the quadrupole kick at time $t = \tau$. An interesting effect occurs at time $t = 2\tau$, where the particles temporarily get in phase again, causing a sudden blip in the centroid signal [2]. This blip is called an echo, and its properties can be traced back to measure diffusion coefficients.

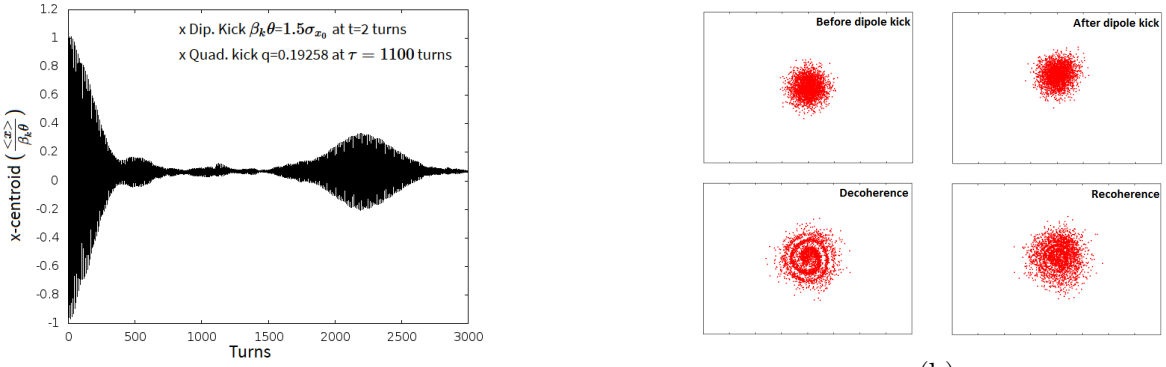

(a) (b)

Figure 1: a) Centroid signal in the IOTA ring, and b) Phase space evolution of the beam

Figure 1, plot (a) shows an echo observed in the IOTA ring around time $t = 2200$ turns, as will be confirmed by the nonlinear theory described in section 3. Plot (b) in Figure 1 shows the phase space evolution of the individual particles.Before the dipole kick, the particles are clustered together in phase space, and the centroid oscillates about zero. After the dipole kick, the particles are displaced vertically by a magnitude θ in the phase space, θ being the bend angle of the kicker. On account of the tune spread, the particles decohere, causing a spiral pattern in phase space, and at time $t = 2\tau$, the particles recluster partially, causing the echo.

3 Nonlinear theory of echoes

According to the current nonlinear theory of echoes, relative echo amplitudes are given by the equation [2]

$$A = \frac{< x >}{\beta_k \theta} \approx \frac{Q}{(1+Q^2)^{3/2}} \tag{3}$$

where $Q = q\omega^{'}\epsilon_f\tau$, $q = \frac{\beta_{quad}}{f}$, f is the focal length of the quadrupole kicker lens, $\omega^{'}$ is the slope of angular betatron frequency vs. action, τ is the time interval between two kicks, and ϵ_f is the final emittance of the beam. Even though there is no direct dependence on dipole kick strength, the final emittance scales as $\frac{\epsilon_f}{\epsilon_0} = 1 + \frac{1}{2}(\frac{\beta_k\theta}{\sigma_x})^2$,where $\beta_k\theta$ is the magnitude of dipole kick, ϵ_0 is the initial emittance, and σ_x is the x RMS of the initial particle distribution. As emittance increases, relative echo amplitude decreases. There are two basic assumptions made about the parameters in the above theory: The time between two kicks is much larger than decoherence time, and the dipole and quadrupole kicks are weak. The exact conditions for weak dipole and quadrupole kicks can be found in reference [3].

From equation (3), the optimum quadrupole strength can be calculated, and maximum echo amplitude occurs when $Q_{opt} = \frac{1}{\sqrt{2}}$. At optimum quadrupole strength, the relative echo amplitude saturates to $A = 0.38$ for reasonable emittances. If a large enough dipole kick is provided, multiple echoes could be observed at $t = 4\tau$,$t = 6\tau$ and so on [2].

4 Simulations of a FODO lattice with octupoles

The first set of simulations was performed on a simple FODO lattice with octupoles. The lattice consisted of 12 FODO cells joined together in a ring through bending magnets. The nonlinear theory of echoes described above was confirmed, and new results on coupling effects were observed that were explored further in the IOTA ring.

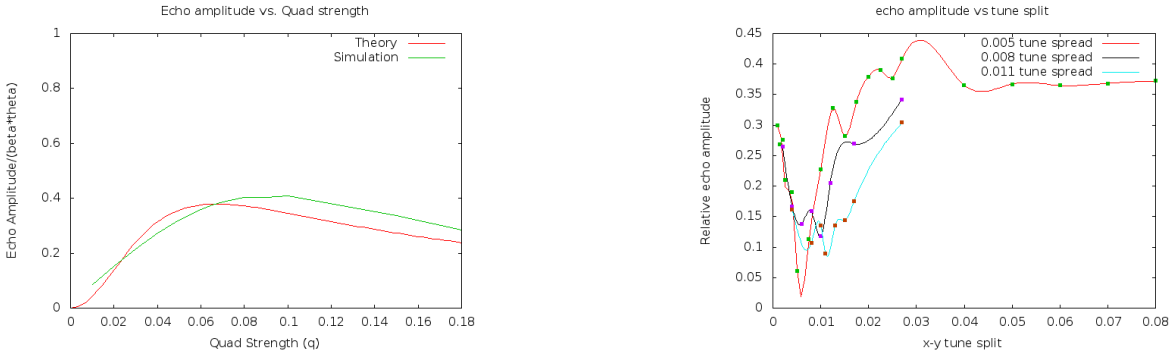

(a) (b)

Figure 2: (a) Echo amplitude vs. quad. strength (Tune split = 0.01, Dipole kick strength = 1.5σ), and (b) Echo amplitude vs. tune split ($\nu_y - \nu_x$) (Quad strength=0.01,Dipole kick strength = 1.5σ)

Figure 2(a) shows how that the variation of echo amplitude as a function of quadrupole strength is in good agreement with theory. Figure 2(b) shows a reduction in echo amplitudes near zero tune splits. This occurs because of coupling. These results will be explored further in the IOTA ring (Section 5.2 and 5.4).

5 Simulations of the IOTA ring

5.1 Layout of the IOTA ring and parameters

The IOTA lattice was simulated in MADX, and the data was analyzed using C++. The beam and ring parameters were chosen to be those of the actual ring, with the addition of dipole and quadrupole kickers in the south straight. The proton beam was kicked in the x plane. The layout of the IOTA ring, and the parameters of the ring are summarized in the figure and tables below [4]. The current pulse width of both kickers should be less than one revolution period ($2\mu s$) to avoid multiple kicks.

The dipole and quadrupole kicks can be calculated using the following formulas:

$$\Delta\theta \approx -\frac{Bl}{(B\rho)}, \quad K = \frac{B'}{(B\rho)} \tag{4}$$

where $\Delta\theta$ is the bend angle of the dipole kicker, B is the field of the dipole, $(B\rho)$ is the rigidity, K is the quadrupole kicker strength, l is the length of the dipole kicker. Knowing the length of the dipole kicker, its bend angle and rigidity allows us to calculate its field. Similarly, knowing the strength of the quadrupole kicker and rigidity allows us to calculate field gradient of the quadrupole.

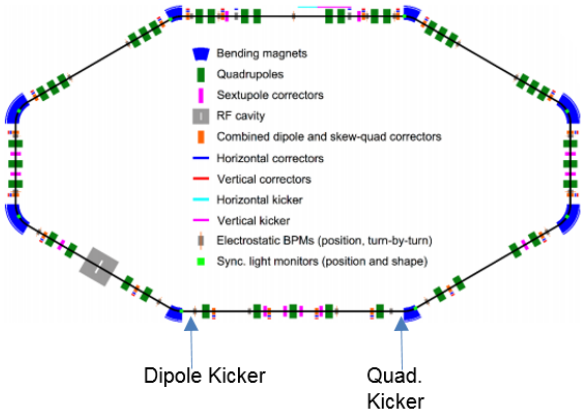

Figure 3: Layout of the IOTA ring

Circumference	40 m
Kinetic Energy	2.5 MeV
Intensity	10^9 protons/bunch
x and y tunes	5.3
Unnorm. x emittance	$4\mu m$
Unnorm. y emittance	$4\mu m$
Dipole Kicker field strength	7 mT
Quad. Kicker Gradient	0.4 T/m
Quad. kicker Field at pole tip(25 mm)	10 mT
Length of Dipole Kicker	0.1 m
Length of quadrupole kicker	0.1 m

5.2 Verification of the nonlinear theory

The predictions made by the nonlinear theory were tested, and the echo simulations are in good agreement with theory. However, the final x emittance predicted by theory does not match simulations. On further observation, it was found that the y emittance, which is expected to stay constant, varies with time. These results can be explained by the fact that when x and y tunes are close to each other, strong coupling (more in section 5.4) causes some energy of the dipole kick to be transferred to the y plane, and the nonlinear echo theory fails to take coupling into account. Hence, in this case, the emittances are different from expected values. However, the square root of the determinant of the covariance matrix, given by [5]

$$\begin{bmatrix} < x^2 > & < xx' > & < xy > & < xy' > \\ < xx' > & < x'^2 > & < x'y > & < x'y' > \\ < xy > & < x'y > & < y^2 > & < yy' > \\ < xy' > & < y'x' > & < yy' > & < y'^2 > \end{bmatrix}$$

obeys the relation $\frac{\sqrt{|Cov.Matrix|}}{\epsilon_0}=1+\frac{1}{2}(\frac{\beta_k\theta}{\sigma_x})^2$. The plots for x,y emittances and the square root of the determinant of the final product are shown below.

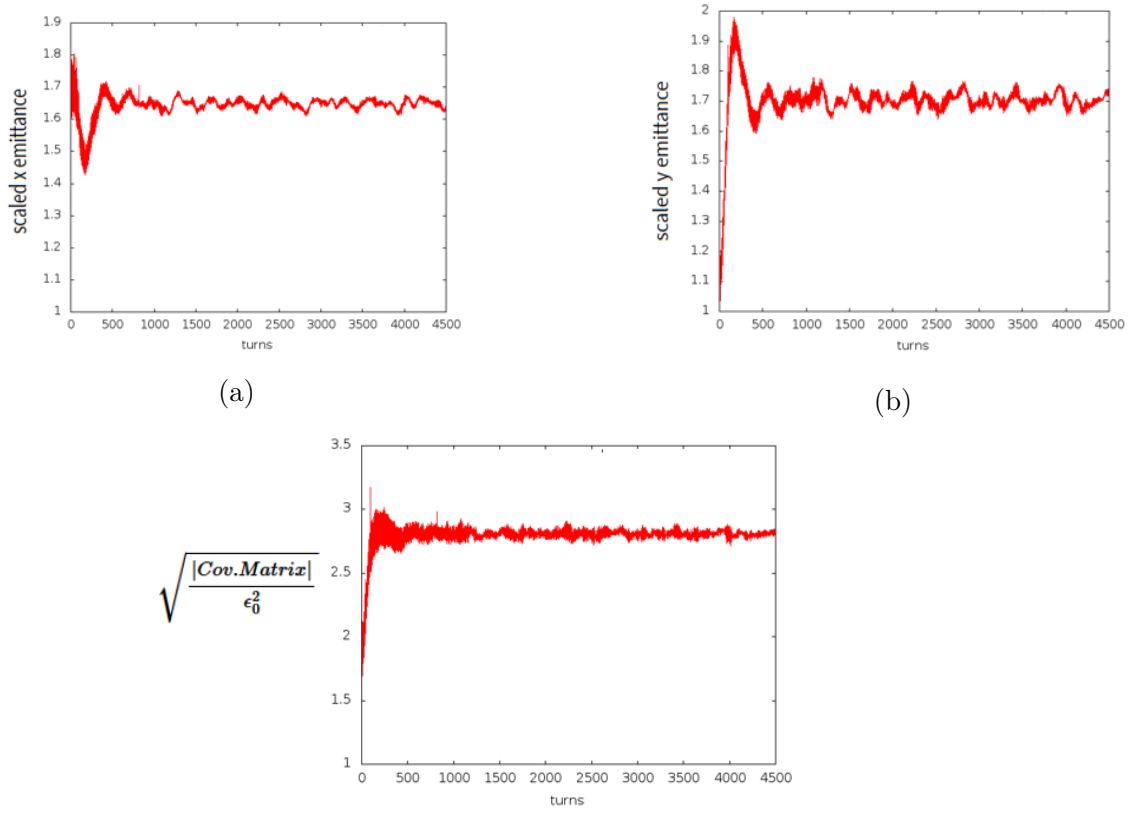

(a) (b)

(c)

Figure 4: a) x emittance, b) y emittance, and c) square root of det. of covariance matrix for a $1.5\sigma_x$ dipole kick

Taking into account coupling and using the square root of the determinant of the covariance matrix, the simulations are in really good agreement with the theory. The plots for echo amplitude as a function of quad. kicker strength, final emittance, and echo amplitude as a function of initial emittance(Figures 5, and 6) are shown below.

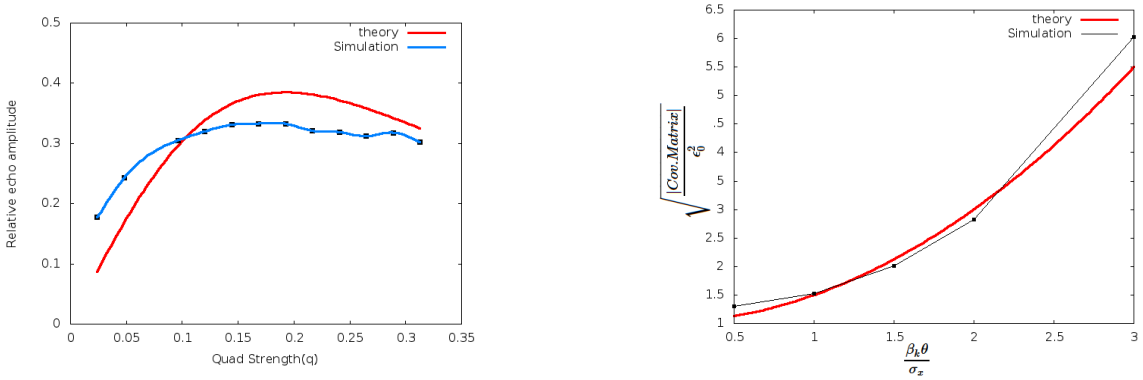

(a) (b)

Figure 5: (a) echo amp. vs. quad. strength, (b) final square root of determinant of covriant matrix vs. dipole kick

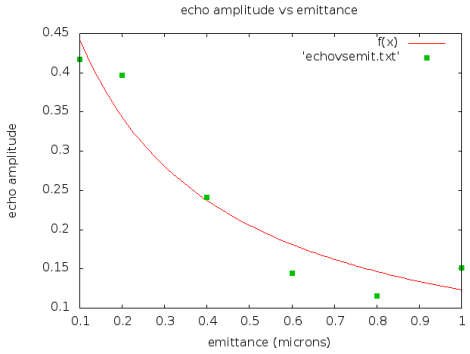

Figure 6: Echo amp. vs. initial emittance

The simulations(Figure 5(a)) show that the echo amplitude reaches a maximum value of 0.335, less than the predicted value of 0.38. This unexpected behavior can also be explained by taking coupling into account. At smaller tune splits, the x and y planes are coupled, and some of the energy from the dipole kick goes into the y plane, and less energy goes into the x plane compared to the no coupling case, leading to a reduction in echo amplitude.

Figure 5(b) shows that the square root of the determinant of the covariance matrix increases with the increase in dipole kick, in accordance with the curve predicted by theory. Figure 6 shows that relative echo amplitude decreases as emittance increases. This is because of the fact that increasing emittance leads to increase in transverse distribution of particles, and thus a larger tune spread than usual, causing suppression of recoherence effect.

5.3 Dynamic Aperture and resonances

Dynamic Aperture is the maximum limit in phase space beyond which particles get lost due to nonlinear fields. It is important to ensure that dynamic aperture of the beam is not too low to minimize particle loss. A way to quantify measurements of dynamic aperture would be to evaluate the expression $\sqrt{(\frac{x}{\sigma_x})^2 + (\frac{y}{\sigma_y})^2}$ and find its minimum value . It is necessary to test robustness of dynamic aperture against longitudinal momentum spread and coupling. As seen from figures 7(a) and 7(b), dynamic aperture does not change by much on introducing longitudinal momentum spread, and is nearly constant for smaller range of tune splits.

When the frequency of oscillation of particles around the ring is an integer(resonance), that would mean the particles arrive at the same phase after they go around the ring. This would lead to propagation of initial errors and a loss of particles. Hence, it is important to select x and y tunes such that they don't drive resonances, since that would lead to loss of a substantial fraction of particles. The IOTA ring has nominal tunes of 5.3 in x and y planes, coinciding with 10^{th} order resonance lines. However, the highest order magnetic field is that due to sextupoles, and sextupoles don't excite 10^{th} order resonances. Sextupoles drive 3^{rd} order resonances, and hence the x-y tune spreads have to be less than 0.03 to avoid this resonance.

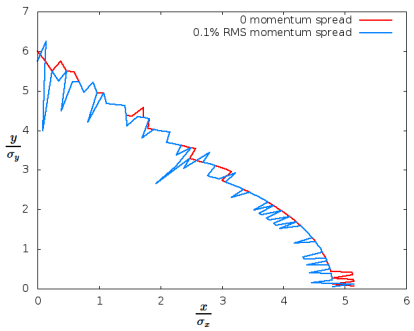

(a)

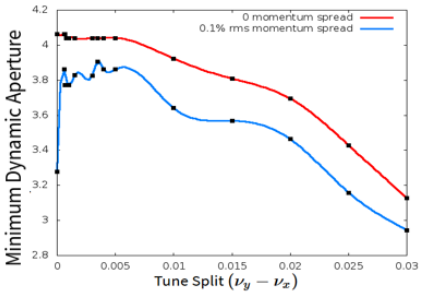

(b)

Figure 7: a) Dynamic Aperture of the IOTA lattice, b) Dynamic Aperture vs. tune split (0 chromaticity)

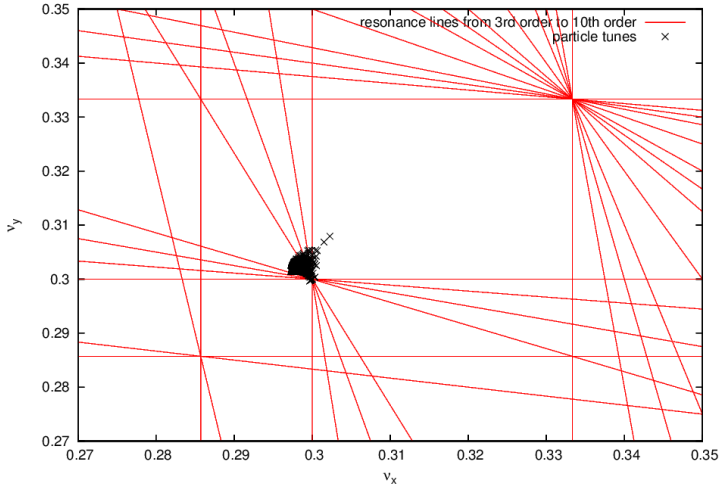

Figure 8: Tune footprint (Nominal tunes 5.3)

5.4 Effects of coupling on echoes

An analogy of weak coupling between pendula helps understand coupling effects on echoes. Two pendula coupled together using a weak spring execute energy transfer between them. Providing a kick to one of the pendula makes it oscillate about equilibrium. After some time, energy transfers to the other pendulum, making it oscillate. The energy oscillates between pendulum 1 and pendulum 2. Energy transfer is maximized when the natural frequencies of two pendula are equal.

Similarly, in any accelerator, when the x and y tunes(frequencies) are close to each other, the dipole kick, even though acting in the x plane, transfers some of its energy to the y plane. This causes individual particle amplitudes to be lesser than the amplitudes in the case where all energy of the kick goes in the x plane, and thus the echo amplitude gets reduced. This phenomenon is called coupling. The closer the tunes are, the stronger the coupling, and the lesser is the echo amplitude. The plots emphasizing consequences of coupling are shown below. Even though lesser nominal tune split leads to stronger coupling, since the particle tunes are different from the nominal tunes due to tune spread, a more direct correlation would be between coupling and the fraction of particles with same tunes.

The plots confirm the prediction that echo amplitude decreases with increase in coupling

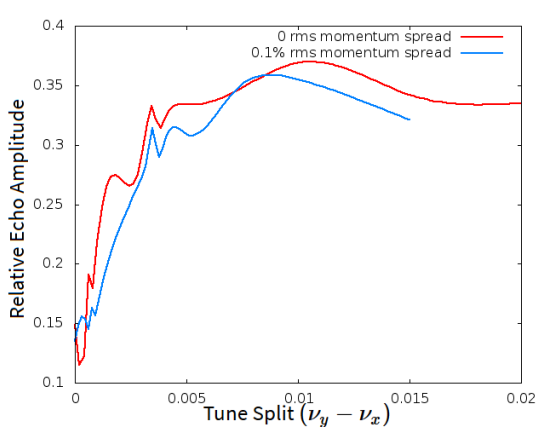

(a)

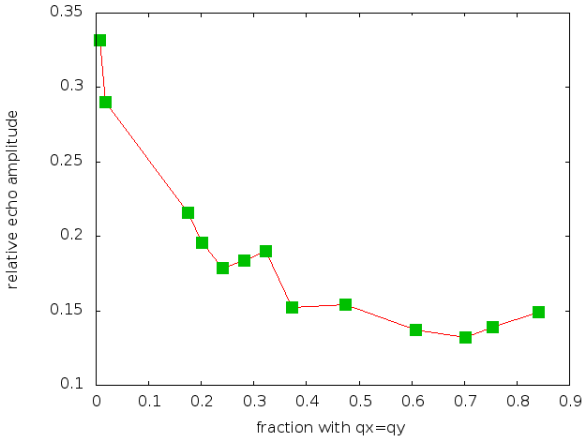

(b)

Figure 9: a) Echo amplitude vs. nominal tune split ($\nu_y - \nu_x$) , b) Echo amplitude vs. fraction of particles with same tunes ($1.5\sigma_x$ dipole kick and 0.19 quad. kick)

and as more tunes line along the diagonal (the positive slope diagonal in figure 7). However, for larger tune splits, echo amplitudes are fairly stable over a large range, making them robust against choice of tunes.

There are two opposing effects in play here. To increase the dynamic aperture and avoid resonance effects, the x and y tunes should be as close as possible to each other, so that particle loss is minimized. However, smaller tune splits lead to a reduction in echo amplitudes, making it difficult to measure them. Hence, the tune split needs to be optimized to take both particle loss and echo amplitude reduction into account.

Other consequences of coupling include increase in decoherence time. As the x and y tunes get closer together, the coupling between the two planes is the strongest, locking the particle motion in coupling resonance, decreasing effective tune spread. The decoherence time is inversely proportional to the tune spread of particles. The larger the tune spread of particles, the easier it is for them to get out of phase with one another, and the smaller the decoherence time is. Hence the decoherence time increases as we get closer to coupling resonance. When the particles move away from resonance, the effective tune spread increases again, and the decoherence time decreases.

5.5 Impact of misalignment and gradient errors

Up until now, the simulations used the bare IOTA lattice, without any errors or nonlinear inserts. To see how robust echoes are against addition of these errors, different misalignment and gradient errors were introduced in all the quadrupoles (independent of each other), and it was found that echoes are robust against addition of misalignment errors,and hence closed orbit errors of up to x RMS of 0.4mm. Apart from that, addition of gradient errors under 0.1% does not change echo amplitudes by a substantial amount. These results show that echoes can still be observed with amplitudes large enough for diffusion measurements even under a more realistic model. The plots of relative echo amplitudes vs. closed orbit errors and gradient errors are shown in Fig. 10.

The plots in Fig 10 show that as the magnitude of the errors increases, the relative echo

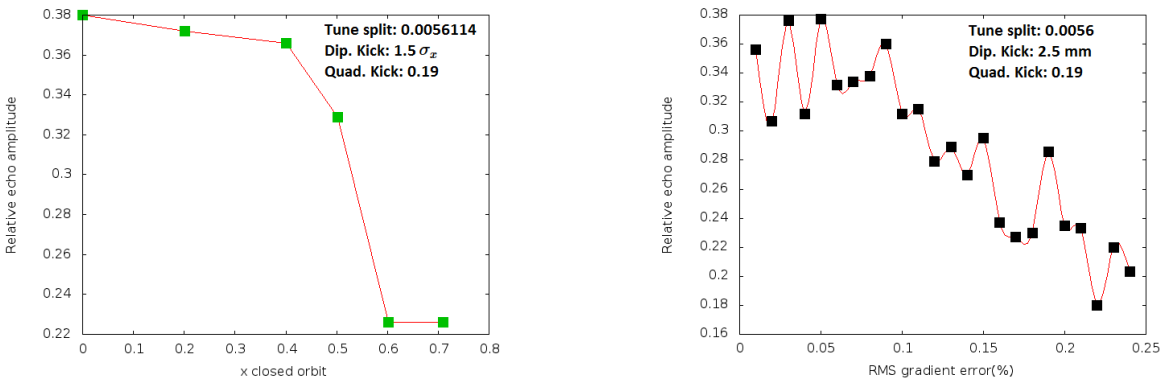

(a) (b)

Figure 10: 1) Relative echo amplitude vs. closed orbit error distortion, 2) Relative echo amplitude vs. gradient errors

amplitude gets suppressed because the recoherence effect is diminished. This happens due to multiple reasons. Firstly, the phase advance is different in each cell, causing symmetry breakdown due to which the recoherence is not fully recovered. Also, errors lead to more tune spread than usual, making it difficult for particles to get back in phase at the echo location. The overall effect is to reduce relative echo amplitudes to values $A < 0.38$ for reasonable emittances.

5.6 Multiple Echoes

If the beam is kicked using a large enough dipole kick strength, the nonlinear theory predicts echoes at $t = 4\tau$, $t = 6\tau$,etc. Using multiple echoes and their properties, we can increase the accuracy of diffusion calculations. However, it is important to keep in mind that the dipole kick should not be too large as to cause substantial particle loss. To reduce particle loss, the initial emittance was reduced to compensate for the effects of larger dipole kick. The dipole kick was increased till we start to get at least two echoes in the IOTA case, and the results are shown below. The echo at $t = 4\tau$ has a lesser amplitude than the echo at $t = 2\tau$, as the recoherence effect is diminished.

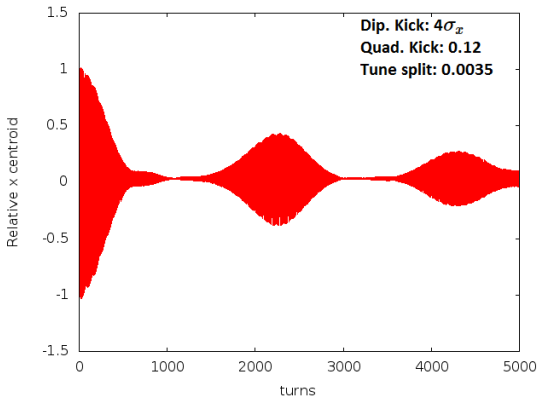

Figure 11: Relative centroid position

6 Conclusions

Echoes generated in the IOTA ring at low intensities have relative amplitudes reaching 0.38, close to the saturation value. Amplitudes of this order are good enough for measuring diffusion and testing integrability quickly. The parameters chosen for dipole and quadrupole kickers are of reasonable values. Another important conclusion that helps keep track of particle loss is that beam can be kicked up to $3\sigma_x$ without losing particles. Echo amplitudes are fairly robust against the choice of tunes (except near zero tune split) and longitudinal momentum spread. Even on introducing gradient and misalignment errors, echo amplitudes were fairly stable over a large range (upto 0.1 % for gradient errors and 0.4mm RMS closed orbit errors). Effects of emittance can be observed through echo amplitudes. Relative echo amplitude reaches values greater than 0.38 at emittances smaller than 0.2 μrad, and decreases as the emittance increases. Overall, the simulations are in good agreement with nonlinear theory. If a large dipole kick is provided, we can observe multiple echoes.

7 Future work

To make the model more realistic, rotation errors should be added so that echo robustness against these errors can be tested. The most important scope for future work lies in using the simulations of coupling effects on echoes to arrive at a general, 2 dimensional theory of echoes that takes into account resonance between the x and y planes. Also, the current intensity of the proton beam (about 100 pc) is low enough so that space charge effects don't need to be taken into account. However, at higher intensities, space-charge affects beam evolution in phase space, and thus echo properties. So increasing beam intensity to take space charge effects into account would help analyze how echoes are affected. Finally, echoes and beam diffusion in the IOTA ring with the nonlinear inserts needs to be calculated.

8 Acknowledgements

I would like to thank my mentor Dr. Tanaji Sen, program director Dr. Peter Garbincius, and the Lee Teng Fellowship in Accelerator Science and Engineering for their support.

9 References

1) G. Valentino, R. Assmann, R. Bruce, F. Burkart, V.Previtali, S. Redaelli, B. Salvachua, G. Stancari, and A.Valishev, Beam diffusion measurements using collimator scans in the LHC, Phys. Rev. ST Accel. Beams 16, 021003 (2013).

2)Tanaji Sen and Yuan Shen Li. 2018. Nonlinear theory of transverse beam echoes. Physical Review Accelerators and Beams 21,021002.

3) Echoes lecture notes, Alex Chao, Stanford University.

4)S. Antipov et al 2017 JINST 12 T03002.

5)Eduard Prat and Masamitsu Aiba. 2014. Four-dimensional transverse beam matrix measurement using the multiple-quadrupole scan technique. Physical Review Accelerators and Beams 17,052801.